PANDER transgenic mice display fasting hyperglycemia and hepatic insulin resistance

Claudia E Robert-Cooperman, Grace C Dougan[1], Shari L Moak, Mark G Athanason, Melanie N Kuehl, Harris Bell-Temin, Stanley M Stevens Jr and **Brant R Burkhardt**

Department of Cell Biology, Microbiology and Molecular Biology, University of South Florida, 4202 East Fowler Avenue, BSF 206, Tampa, Florida 33620, USA
[1]Department of Pediatrics, University of South Florida, 12901 Bruce B. Downs Boulevard, MDC 62, Tampa, Florida 33612, USA

Correspondence should be addressed to B R Burkhardt
Email
bburkhardt@usf.edu

Abstract

PANcreatic-DERived factor (PANDER, FAM3B) is a novel protein that is highly expressed within the endocrine pancreas and to a lesser degree in other tissues. Under glucose stimulation, PANDER is co-secreted with insulin from the β-cell. Despite prior creation and characterization of acute hepatic PANDER animal models, the physiologic function remains to be elucidated from pancreas-secreted PANDER. To determine this, in this study, a transgenic mouse exclusively overexpressing PANDER from the endocrine pancreas was generated. PANDER was selectively expressed by the pancreatic-duodenal homeobox-1 (*PDX1*) promoter. The PANDER transgenic (PANTG) mice were metabolically and proteomically characterized to evaluate effects on glucose homeostasis, insulin sensitivity, and lipid metabolism. Fasting glucose, insulin and C-peptide levels were elevated in the PANTG compared with matched WT mice. Younger PANTG mice also displayed glucose intolerance in the absence of peripheral insulin sensitivity. Hyperinsulinemic–euglycemic clamp studies revealed that hepatic glucose production and insulin resistance were significantly increased in the PANTG with no difference in either glucose infusion rate or rate of disappearance. Fasting glucagon, corticosterones, resistin and leptin levels were also similar between PANTG and WT. Stable isotope labeling of amino acids in cell culture revealed increased gluconeogenic and lipogenic proteomic profiles within the liver of the PANTG with phosphoenol-pyruvate carboxykinase demonstrating a 3.5-fold increase in expression. This was matched with increased hepatic triglyceride content and decreased p-AMPK and p-acetyl coenzyme A carboxylase-1 signaling in the PANTG. Overall, our findings support a role of pancreatic β-cell-secreted PANDER in the regulation of hepatic insulin and lipogenic signaling with subsequent impact on overall glycemia.

Key Words
- insulin resistance
- mouse
- liver
- pancreas
- whole animal physiology

Journal of Endocrinology (2014) **220**, 219–231

Journal of Endocrinology

Introduction

PANcreatic-DERived factor (PANDER, FAM3B) is a 235-amino acid protein preferentially secreted and expressed from pancreatic α and β cells, and to lower levels in the intestine and prostate (Zhu *et al*. 2002, Cao *et al*. 2003). In contrast to earlier findings, other investigators have detected the presence of PANDER in stomach, muscle, liver, and brain tissues (Li *et al*. 2011). The family with sequence similarity 3 (FAM3) was identified using a

http://joe.endocrinology-journals.org
DOI: 10.1530/JOE-13-0338

Published by Bioscientifica Ltd.

computational algorithm known as ostensible recognition of folds (ORF; Aurora & Rose 1998). This search identifies protein sequences that may form a four-helix-bundle structure based on predicted secondary structure that is typically found in many cytokines. From ORF, the predicted structure of FAM3B (name was changed to PANDER in 2003) was determined to be a four-helix bundle. Despite this initial prediction, recent crystallographic studies of secreted PANDER have revealed that the true structure is a globular β-β-α fold, demonstrated by the presence of two antiparallel β sheets lined by three short helices packed to form a highly conserved water-filled cavity (Johansson *et al*. 2013). This unique structure continues to be preserved for other members of the FAM3 group, and thereby potentially constitutes a new class of signaling molecules distinctly different from other known cytokines or hormones.

With regard to biological function, *in vitro* studies revealed the increased production of PANDER mRNA and protein under glucose stimulation of the pancreatic β-cell, but not the α-cell (Burkhardt *et al*. 2005, Yang *et al*. 2005, Wang *et al*. 2008). In contrast, insulin stimulates PANDER secretion from the pancreatic α-TC1-6 cell line and appears to be located in an intracellular compartment distinct from glucagon (Carnegie *et al*. 2010). Palmitic acid has also been reported to induce PANDER mRNA and protein expression in a dose and time dependent manner in a pancreatic β-cell line (Chen *et al*. 2011, Xiang *et al*. 2012). In addition, the critical pancreatic β-cell-specific transcriptional factor, pancreatic-duodenal homeobox domain-1 (PDX1), interacts and increases the expression of the *PANDER* promoter (Burkhardt *et al*. 2008).

PANDER's location and regulation have led to a potential relationship with glucose regulation, and several animal models have been derived to study this with some conflicting results. Wilson *et al*. (2010) evaluated hepatic *PANDER* overexpression achieved through adenoviral delivery. This model revealed fasting hyperglycemia, hyperinsulinemia, and elevated corticosterone levels. Li *et al*. (2011) derived a similar adenoviral-delivered overexpressing model with different results, and did not observe glucose intolerance, fasting glycemia, or elevated corticosterone levels. However, liver and serum triglyceride content was increased along with serum insulin levels, as compared with WT mice. Differences between the studies may certainly be attributed to alterations in time and dose of adenoviral delivery and subsequent PANDER expression. Although prior animal models of PANDER have certainly revealed useful information, none provided a physiologically selective model of PANDER expression to focus on its function in the context of the observed *in vivo* tissue distribution of PANDER.

Therefore, to further elucidate the physiologic role of pancreas-secreted PANDER *in vivo*, our laboratory has created and phenotyped the only transgenic mouse model (PANDER transgenic, PANTG) with tissue-specific PANDER overexpression and secretion from the endocrine pancreas. Our metabolic phenotyping and proteomic analysis strongly indicate that endocrine-specific overexpression of PANDER impacts hepatic glycemic output and lipid regulation.

Materials and methods

Transgenic mouse generation and genotyping

The *Fam3b* (PANDER) gene cloned into the pCR2.1 cloning vector (Life Technologies) was kindly provided by GlaxoSmithKline. The *Pander* gene was excised and ligated downstream of the *Pdx1* promoter which drives the expression exclusively in the endocrine tissue of the pancreas. This vector was obtained from Dr Maureen Gannon, Vanderbilt University (Samaras *et al*. 2002). B6SJLF (strain generated from a cross between C57BL/6J females and SJL/J males) transgenic mice were produced according to the protocol of the University of Pennsylvania Transgenic and Chimeric Mouse Facility. During the course of this investigation, the laboratory and animal colony were moved to the University of South Florida (USF) from the Children's Hospital of Philadelphia. Frozen embryos of the PANTG were shipped to the Moffitt Stabile Vivarium on the campus of USF and implanted into pseudo pregnant females for subsequent rederivation of murine colony. Animals were fed standard chow from Purina and given water *ad libitum*. All animals were handled according to the guidelines established by the Institutional Animal Care and Use Committee at the University of South Florida and Children's Hospital of Philadelphia before relocation. Offspring were screened by PCR to confirm transgenic integration using primers specific (forward 5′-GCT GGA CAG GGG CAC GTC AGG AAT GAG CTC-3′ and reverse 5′-TAC TCT GAG TCC AAA CCG GGC CCC TCT GCT-3′) for the β-globin intron and PANDER transgene resulting in a 300 bp transgene-specific PCR product amplified from genomic DNA isolated from tail tissue (DNeasy Kit, Qiagen). All animals were born normally at the expected Mendelian frequency. Male mice aged 8 weeks to 8 months were evaluated in this study. Relative PANDER expression was determined by RT-PCR

http://joe.endocrinology-journals.org
DOI: 10.1530/JOE-13-0338

Published by Bioscientifica Ltd.

and western analysis as described previously (Robert-Cooperman *et al*. 2010).

RT-PCR and western blot

Transgenic and WT mouse pancreatic islets were isolated by collagenase digestion followed by a Ficoll gradient, as described previously (Robert-Cooperman *et al*. 2010). Islet lysate was then evaluated for PANDER expression via RT-PCR and western analysis, as described previously (Robert-Cooperman *et al*. 2010). Western blotting analysis for hepatic insulin signaling molecules was carried out by initially isolating protein from snap–frozen livers, using the tissue protein extraction reagent (TPER; Thermo Fisher Scientific, Rockford, IL, USA). Hepatic lysate (typically 20–40 μg) was analyzed by SDS–PAGE (Bio-Rad Pre-Cast 12% TGX gels, Bio-Rad) and subsequently transferred onto PVDF membrane using the iBlot semi-dry transfer system (Invitrogen). Western blots were detected with antibodies for phosphorylated and total proteins of AMPK and acetyl coenzyme A carboxylase-1 (ACC; Cell Signaling, Danvers, MA, USA) diluted at 1:1000 in commercial StartBlock blocking buffer (Thermo Fisher Scientific). Detection was performed using peroxidase-conjugated secondary antibodies at 1:10 000 using chemiluminescence detection reagents and signals were visualized using the LAS 3000 Intelligent Dark Box (Fujifilm, Stamford, CT, USA). Protein levels were normalized to glyceraldehyde 3-phosphate dehydrogenase (GAPDH; Cell Signaling). Densitometry analysis was performed using Image J (version 1.45) analysis.

Immunohistochemistry of transgenic islets

Pancreatic sections from PANTG and WT mice were fixed for 24 h in formalin and embedded in paraffin as performed by Children's Hospital of Philadelphia pathology core. The sections were stained using aldehyde fuchsin or hematoxylin and eosin (H&E) stains. Immunostaining for insulin was performed with a guinea pig anti-insulin primary antibody (Dako, Carpinteria, CA, USA) and anti-guinea pig cy3 conjugated secondary antibody. Glucagon staining was done with a rabbit anti-glucagon primary antibody (Dako) and anti-rabbit cy2 conjugated secondary antibody. PANDER staining was performed using a rabbit polyclonal PANDER antibody as described previously, followed by an anti-rabbit biotinylated secondary antibody which complexes with HRP-conjugated streptavidin molecules in a subsequent wash (Cao *et al*. 2003).

PANDER ELISA

To measure the levels of PANDER in the serum, a commercial ELISA (Life Sciences Advanced Technologies, Cat No. E03P0025, St Petersburg, FL, USA) was carried out on the blood sample collected from the tail vein of PANTG and WT mice during fasted (16 h overnight) and fed (4 h exposure to food following overnight fast) conditions, according to manufacturer's instructions.

Animal growth measurement

WT and PANTG mice at 3–4 months of age were weighed (Beckman Digital Scale) in the morning upon overnight fasting and again at 5–6 months of age before stimulation testing. Weight in grams was averaged for each group and compared at the two designated time points ($n=40$).

Glucose tolerance testing

Mice were fasted overnight (16 h) in a cage with fresh bedding before glucose tolerance testing (GTT). Blood glucose (BG) was measured immediately before glucose injection and then at 15, 30, 60, 90 and 120 min following i.p. injection of glucose at a concentration of 2 g/kg body weight. Blood was collected via tail vein and concentration of glucose was measured using a True Track Smart System glucometer (Home Diagnostics, Inc., Fort Lauderdale, FL, USA).

Insulin tolerance testing

Mice were fasted for 4 h in a cage with fresh bedding before insulin tolerance testing (ITT). BG levels were measured immediately before i.p. injection of insulin at a concentration of 1 U/kg of body weight. BG was then measured as above at 0, 15, 30, 60, 90 and 120 min post injection.

Hyperinsulinemic–euglycemic clamp

Clamp studies were performed by the University of Pennsylvania Mouse Phenotyping Core as described previously (Robert-Cooperman *et al*. 2010). For calculation, rates of whole-body glucose appearance and uptake were determined as the ratio of the H^3 glucose infusion rate (GIR) (disintegrations per min/min) to the specific activity of plasma glucose (dpm/μmol) during the final 30 min of clamps. Hepatic glucose production (HGP) during the hyperinsulinemic–euglycemic clamps (HEC)

http://joe.endocrinology-journals.org
DOI: 10.1530/JOE-13-0338

Published by Bioscientifica Ltd.

was determined by subtracting the GIR from the whole-body glucose appearance.

Serum collection for hormones and triglyceride assays

Mice were fasted for 16 h before serum collection. Blood was obtained by vein puncture and free flow collection in SarStead collection tubes. The whole blood samples were centrifuged for 5 min and the serum was separated to a new collection tube. The hormone analytes were measured using Luminex Multiplex Platform (MAGPIX), with commercial mouse endocrine panel (Millipore Kit MMHMAG-44K; EMD Millipore, Billerica, MA, USA), ENZO EIA assay kit for corticosterone, and Abcam Triglyceride Kit.

Stable isotope labeling of amino acids to cell culture

Isolated liver lysate was prepared from PANTG and WT male mice ($n=6$ per group) during random fed conditions. Livers were homogenized in TPER buffer (Thermo Fisher Scientific) followed by high-speed centrifugation. Ethanol-treated AML-12 cells were utilized as a surrogate cell line for comparing protein, as described previously (Monetti *et al.* 2011). The AML-12 cells were heavy labeled by culturing in a medium containing $_{13}C_6$ L-lysine-2-HCl and $_{13}C_6$ L-arginine-HCl followed by homogenization in MPER buffer (Thermo Fisher Scientific, Rockford, IL, USA) followed by high-speed centrifugation. Supernatants were collected and protein concentration was quantified (Pierce BCA protein assay). Equivalent amount of liver protein was then spiked with equal mass of protein from AML-12s. The spiked mixture was solubilized using FASP protein digestion kit (Protein Discovery, Knoxville, TN, USA). The six samples derived from PANTG and WT livers, respectively, were then batched and both samples were desalted before fractionation using an automated CXS column. Nine fractions were selected for both PANTG and WT mice and subsequently dissolved in 1% aqueous formic acid for evaluation by mass spectrometry (LTQ Orbitrap XL™ Hybrid Ion Trap-Orbitrap Mass Spectrometer; Thermo Fisher Scientific). Data were normalized and analyzed using the Ingenuity Pathway Analysis (IPA) program. A total of 1640 proteins were confidently identified and quantitated. Relative changes in the levels of identified proteins were determined by the ratio of PANTG to that of WT and normalized to Tubulin B5. Of those, 88 protein groups were upregulated and nine were downregulated ($P<0.05$ for both groups). The distribution of ratios of all quantitated proteins indicated excellent representation of the proteome between PANTG and WT ratio relative to that of AML-12 cells

Statistical analysis

Statistical analysis of the data was performed using GraphPad Prism software (La Jolla, CA, USA). Data are shown as mean ± S.E.M. Statistical significance of differences between groups was analyzed by unpaired Student's *t*-test. A P value of <0.05 was considered significant.

Results

Endocrine pancreas-specific PANDER overexpression in the PANTG

A 1 kb fragment of the PDX1 promoter was used to drive PANDER overexpression specifically in the endocrine tissue of the pancreas (Fig. 1A). This region of PDX1 has been extensively characterized and demonstrated to govern endocrine-specific expression (Melloul *et al.* 2002). The construct also contains an *Hsp68* cassette that functions as a basal promoter, as the *Pdx1* promoter lacks a TATA box. A β-globin intron fragment and polyA cassette flanking PANDER was incorporated to promote RNA stability (Fig. 1A). Following blastocyst injection (performed by University of Pennsylvania Transgenic Facility) and selection, a founder line was established that demonstrated the highest levels of *Pander* overexpression. RT-PCR (Fig. 1B) and western blot (Fig. 1C) analysis demonstrated an approximate eight- to tenfold increase in *Pander* expression in pancreatic islets from 2-month-old PANTG as compared with WT mice. As expected, the mature (26 kDa) and secreted (23 kDa) forms of the PANDER protein were both increased in the PANTG pancreatic islets (Fig. 1C). Increased *Pander* expression from the PANTG islets was also observed in older mice aged 5–7 months (data not shown). Due to detection limitations of our current antibody, the precise amount of circulating serum PANDER is unknown. Islets isolated from the PANTG secrete significantly higher quantities of PANDER upon glucose stimulation than WT islets (Yang *et al.* 2005). However, we also wanted to confirm that increased PANDER levels were only found within the endocrine pancreas. Immunohistochemical analysis of pancreatic sections from PANTG and WT mice revealed increased *Pander* expression specifically to the endocrine pancreas and not to the surrounding exocrine tissue (Fig. 1D). Due to previous data indicating that PANDER can induce apoptosis in pancreatic β-cell (Cao *et al.* 2003, 2005), morphological differences between PANTG and WT pancreatic islets were

http://joe.endocrinology-journals.org
DOI: 10.1530/JOE-13-0338

Published by Bioscientifica Ltd.

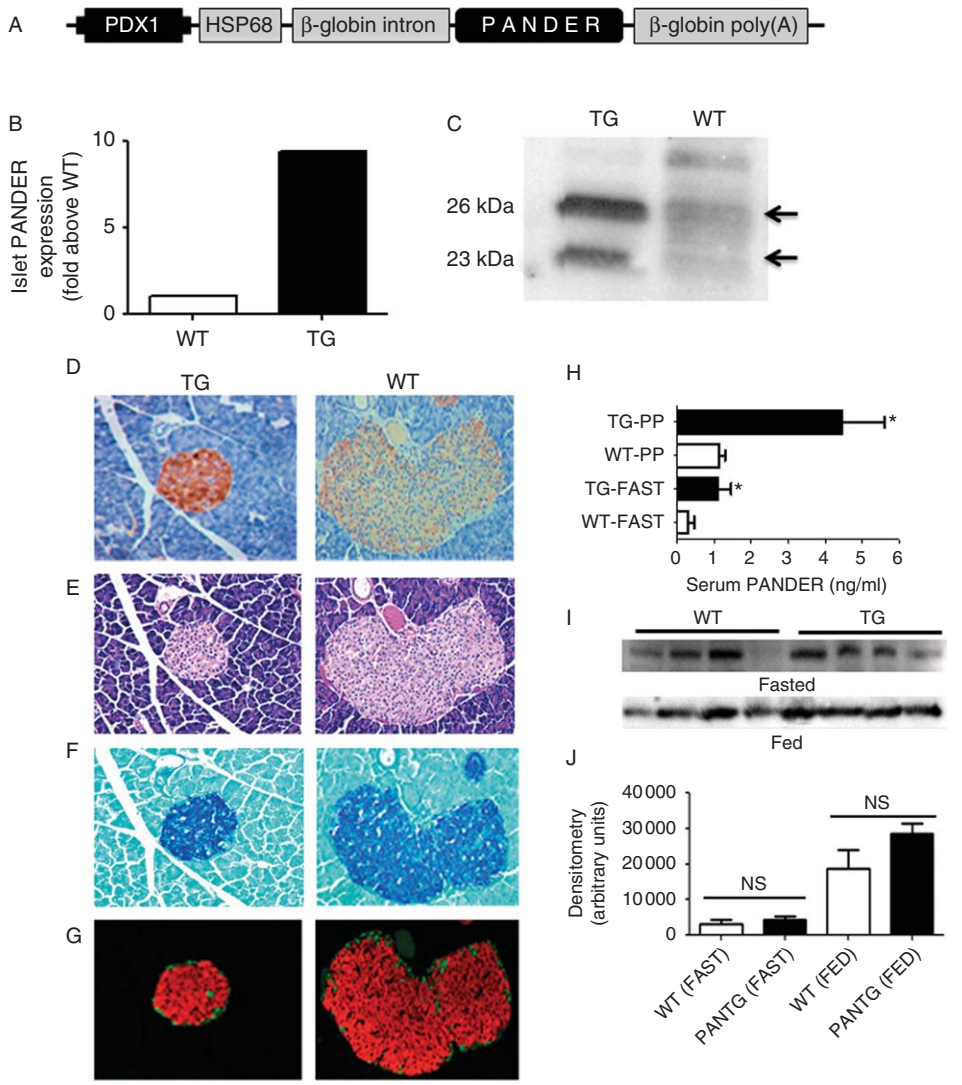

Figure 1

Generation and characterization of the PANDER transgenic (PANTG) mouse. (A) Schematic diagram of the PDX1-PANDER targeting plasmid generated to produce the PANTG. A 1 kb fragment of the *Pdx1* promoter was employed to drive the expression of PANDER in the endocrine tissue of the pancreas. Further features of the plasmid included an *Hsp68* cassette containing a TATA box and functioning as a basal promoter, a β-globin intron to increase RNA stability, and a β-globin polyadenylation signal to promote mRNA stability and inhibit degradation. The following phenotypic descriptions were performed in mice aged 2 months. (B) RT-PCR analysis of RNA isolated from pancreatic islets obtained from WT and PANTG mice. (C) Western analysis of PANDER detection from protein extracted from WT and PANTG isolated islets. Top and bottom arrows indicate full-length (26 kDa) and secreted (23 kDa) forms of PANDER. (D, E, F, and G) Immunohistochemistry performed on matched sections of whole pancreas sections isolated from 2-month old male PANTG (left panels) and WT (right panel) mice. Evaluations of pancreatic islets from older mice aged 5–7 months demonstrated similar results (data not shown). Sections were stained with (D) PANDER antibody, (E) H&E, (F) aldehyde fuchsin, and (G) immunofluorescence with anti-insulin (red) and anti-glucagon (green) antibodies. (H) ELISA measured levels of PANDER (ng/ml) in the serum of overnight fasted (FAST) and post-prandial (PP, 4 h re-feed) male PANTG and WT mice ($n=3$–4 for all groups). (I) Livers were collected from fasting and fed PANTG and WT mice and evaluated by western analysis for PANDER expression as previously described in Materials and methods. Approximately 100 μg was loaded per lane. Lanes 1–4 and 5–8 are from male 7-month-old WT and PANTG mice, respectively. Top half shows representative immunoblot from fasting mice and lower half from fed mice with 100 μg of hepatic lysate per lane. (J) Densitometric analysis of above immunobot as determined by ImageJ. Quantitative values are expressed as means±S.E.M. NS, not significant ($P>0.05$), *$P<0.05$ by Student's *t*-test.

evaluated. These differences included islet size, changes in secretory granules or localization of insulin and glucagon. Therefore, pancreatic islets were assessed using immunohistochemistry for various morphological changes. Staining with hematoxalin and eosin and aldehyde fuchsin showed normal islet and pancreatic morphology with no lymphocytic infiltrate in PANTG mice (Fig. 1E and F). The islets were comparable in size and

http://joe.endocrinology-journals.org
DOI: 10.1530/JOE-13-0338

Published by Bioscientifica Ltd.

shape upon microscopic evaluation. Insulin distribution in PANTG mice when visualized with aldehyde fuchsin staining was similar with that in WT mice. Localization of insulin and glucagon within islets was comparable between PANTG and WT mice as visualized with immunofluorescence (Fig. 1G). Insulin-expressing cells were located throughout the islet core with glucagon-expressing cells mainly within the mantle or periphery. Hence, at the microscopic level, islet morphology in PANTG mice was similar to WT with PANDER overexpression localized to the endocrine pancreas.

To measure PANDER levels in the blood, serum was collected from fasting and fed PANTG and WT mice and evaluated by a recently developed commercial ELISA for the detection of murine PANDER (Life Sciences Advanced Technologies). In general, circulating PANDER in both the fasted and fed states was approximately fourfold higher in the PANTG as compared with matched WT serum (Fig. 1H). Another critical tissue with regard to PANDER expression has been the liver. Therefore, hepatic PANDER levels were examined by western analysis and did not reveal a significant difference between both groups (Fig. 1I and J). However, it should be noted that a non-statistical trend of increased PANDER levels was observed in the PANTG as compared with the WT during fed conditions (Fig. 1J).

Increased fasting glucose and insulin levels in the PANTG mouse

To initially characterize the impact of overexpressed endocrine-specific PANDER on glycemia, glucose levels were measured in PANTG mice following an overnight fast. PANTG mice revealed a significantly elevated BG at 2 months of age compared with WT littermates, with values of 238 mg/dl±29 vs 153 mg/dl±8, respectively, with $P<0.05$ as seen in Fig. 2A. The difference in fasting glycemia was diminished over time due to WT group (6 months of age) having increased glucose levels potentially attributed to age-dependent insulin resistance (Fig. 2A). Significantly higher ($P<0.001$) glycemic values were measured from the PANTG when measuring across both age groups (PANTG 233.8±18.6 vs WT 178.1±8.8, $P<0.001$). To further uncover potential mechanisms of the observed fasting hyperglycemia, we measured the levels of the various hormones of insulin, C-peptide, glucagon, leptin, and resistin. PANTG displayed a significant elevation in insulin compared with WT; 619.3 pg/ml±165.6. vs 179.6 pg/ml±94.4, respectively ($P<$ 0.05) along with C-peptide levels compared with WT; 1629 pg/ml±394 vs 493 pg/ml±246, respectively ($P<0.05$) (Fig. 2B). No significant differences were observed for glucagon, resistin, or leptin. In addition, corticosterone values were also measured and found to be similar with that of WT mice (data not shown).

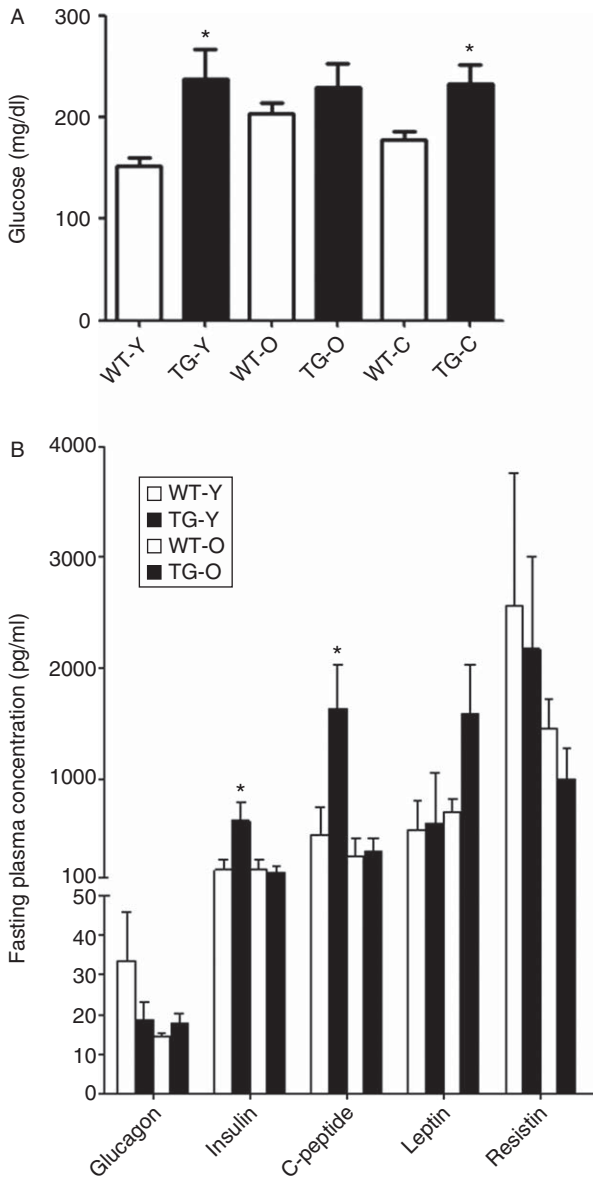

Figure 2
Fasting glycemic and hormonal evaluation of PANTG. (A) Fasting blood glucose levels were measured in male PANTG and WT mice at 3 months of age (designated as TG-Y and WT-Y denoting younger mice) and 6 months of age (designated as TG-O and WT-O denoting younger mice) ($n=20$). (B) Fasting hormonal levels of glucagon, insulin, C-peptide, and resistin were measured in male PANTG and WT mice from plasma by MAGPIX Luminex Assays using the Mouse Endocrine Panel (Millipore) ($n=6$). Values are expressed as means±S.E.M. *$P<0.05$ by Student's *t*-test.

http://joe.endocrinology-journals.org
DOI: 10.1530/JOE-13-0338

Published by Bioscientifica Ltd.

In summary, the initial phenotyping of the PANTG demonstrated increased fasting glycemic and insulinemic levels in the absence of increased glucagon or corticosterone.

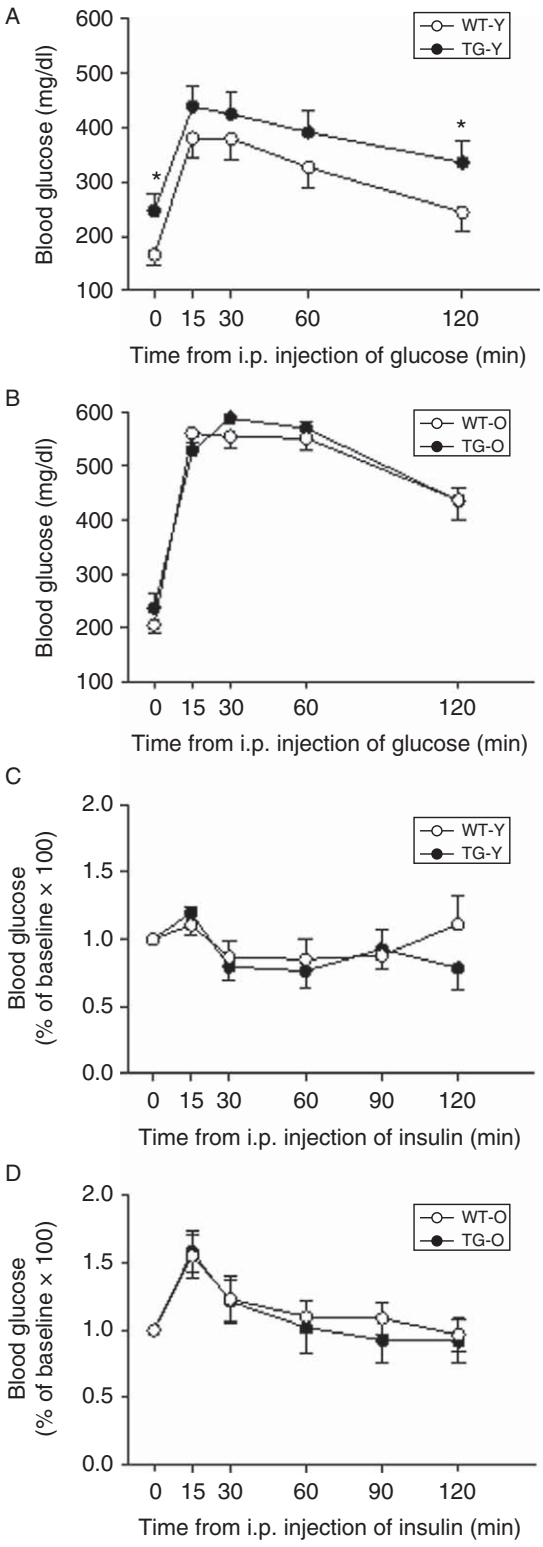

Glucose intolerance in PANTG

To evaluate the role of PANDER during fed conditions, PANTG mice were examined during fed or insulin-stimulated conditions. GTT's demonstrated higher BG levels at completion of the 2 h timed test in PANTG vs WT male mice aged 3 months ($P<0.05$) (Fig. 3A). However, the % glycemic change from baseline was not significantly different between both groups at the conclusion of the GTT (PANTG 156±18% vs WT 155±24.7%, not significant, data not shown). Differences in glucose intolerance diminished over time as indicated by GTT performed on 6-month-old mice, but both groups showed elevated glucose levels during the course of GTT as compared with the younger cohort (Fig. 3B). To evaluate peripheral insulin sensitivity, ITTs were performed. ITT results demonstrated similar peripheral insulin sensitivity for the PANTG and WT mice in both age groups (Fig. 3C and D). In general, PANTG mice demonstrated temporal-dependent glucose intolerance without the presence of peripheral insulin resistance.

Hepatic insulin resistance in PANTG

To further investigate the potential mechanism for the observed fasting hyperglycemia and glucose intolerance, HEC studies were performed to further evaluate insulin sensitivity. GIR and rate of glucose disappearance (Rd) were similar for both PANTG and WT mice and indicated no significant differences in peripheral insulin sensitivity based on the GIR (Fig. 4A) and Rd (Fig. 4B). However, differences were observed with regard to the evaluation of hepatic insulin sensitivity. During the HEC, PANTG mice demonstrated a lower percent suppression and higher HGP as compared with WT mice ($P<0.05$) (Fig. 4C and D). Taken together, these results indicate that pancreas-specific overexpressed PANDER can decrease hepatic

Figure 3
Metabolic studies of PANTG mouse. Glucose tolerance testing was conducted following 16 h fast by an i.p. injection of glucose at 2 g/kg with measuring plasma glucose concentration at times indicted ($n=20$). Values are expressed as means±S.E.M. *$P<0.05$ by Student's t-test. (A) GTT performed at 3 months of age (WT-Y and TG-Y). (B) GTT performed at 6 months of age (WT-O and TG-O). Insulin tolerance tests were conducted by i.p. injection of mice with insulin at 1 unit/kg and measuring glucose concentration at indicated time points. Results are shown as percentage baseline glucose concentration measured at time point 0 ($n=20$). (C) ITT performed at 3 months of age (WT-Y and TG-Y). (D) ITT performed at 6 months of age (WT-O and TG-O).

http://joe.endocrinology-journals.org
DOI: 10.1530/JOE-13-0338

Published by Bioscientifica Ltd.

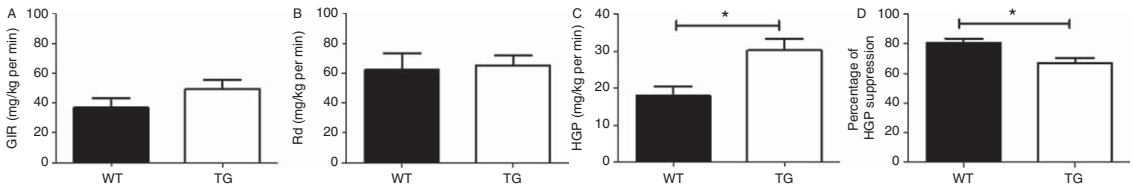

Figure 4
Hyperinsulinemic–euglycemic clamp studies in PANTG. (A) Mean steady state glucose infusion rate (GIR) during HEC ($n=8$). (B) Rate of glucose disposal (Rd) during HEC. (C) Hepatic glucose production (HGP) during clamp conditions. (D) Percentage of HGP suppression during clamp conditions. Male PANTG mice aged 3 months were evaluated ($n=6$–8). Values are expressed as means ± S.E.M. *$P<0.05$ by Student's *t*-test.

insulin sensitivity but not peripherally and alludes to a liver-specific role of PANDER.

Hepatic SILAC analysis of PANTG demonstrates increased gluconeogenic and lipogenic predicted networks

Our initial characterization of the PANTG revealed increased fasting and post-prandial glycemic levels in the absence of peripheral insulin resistance but in the presence of hepatic insulin resistance. Therefore, we then investigated critical hepatic insulin signaling molecules via a comprehensive proteomic approach known as stable isotope labeling of amino acids in cell culture (SILAC). This quantitative proteomic strategy metabolically labels the entire proteome and allows for identification and network elucidation by mass spectrometry analysis and has become a highly useful and relatively novel tool to identify complex protein mixtures, signaling cascades, and regulated protein modifications (Kruger *et al.* 2008, Monetti *et al.* 2011). Total protein isolate was prepared from extracted livers from PANTG and WT mice ($n=6$ per group) obtained during fed conditions. Following processing and SILAC analysis, ~1640 proteins were identified and quantitated. Data were normalized and analyzed using the IPA program. Relative changes in the levels of identified proteins were determined by the ratio of PANTG to that of WT and normalized to proteomic expression of Tubulin B5. Of those, 88 protein groups were upregulated and nine were downregulated ($P<0.05$ for both groups). IPA of the differentially expressed proteins identified lipid metabolism as one of the top associated network functions as significantly upregulated (20 total proteins with $P=9.46\times10^{-6}$) with an overall score of 57 (score of 2 is significant) (Fig. 5A). Further IPA analysis identified quantity of triacylglycerol that is predicted to be in an increased state (*z*-score of 2.4) with a genetic network of interacting proteins consisting of fatty acid binding protein (FABP1), protein kinase A type II-β regulatory subunit (PRKAR2B), phosphoenol-pyruvate carboxykinase (PEPCK), sterol carrier protein (SCP2), acetyl CoA synthetase (ACSL1), and ectonucleoside triphosphate diphosphohydrolase 5 (ENTPD5) (Fig. 5B and C). Of those identified to promote increased triglyceride production, four revealed to molecularly interact as determined by IPA (Fig. 5C). Overall, SILAC identified a proteomic profile within the PANTG liver of increased lipid metabolism and increased PEPCK (gluconeogenic) expression, supporting the observed results obtained with both the HEC and SILAC analysis.

PANTG mice display elevations in liver triglyceride content

HEC and SILAC results of the PANTG strongly suggested an impact in hepatic signaling pathways, with potential alterations in triglyceride content and potential signaling molecules. Therefore, we measured hepatic triglyceride and glycogen content. Hepatic triglycerides were elevated, while glycogen content was significantly decreased in the livers of the PANTG mice as compared with WT (Fig. 6A and B, $P<0.05$). Significant differences in body weight were not observed between PANTG and WT mice at either age (Fig. 6C). With the observed pleiotropic PANDER-induced effects on hepatic triglyceride, glycogen and hepatic insulin signaling, we evaluated the potential of PANDER altering the expression of AMPK and it's downstream target of ACC. Western blot analysis of PANTG livers examined in the fasted and insulin-stimulated conditions revealed an overall trend of decreased phosphorylation of p-AMPK and corresponding p-ACC (Fig. 6D and E). However, statistical significance was only observed during fasting conditions of decreased p-ACC and insulin-stimulated conditions for p-AMPK of the PANTG (Fig. 6F, G, H, and I). Therefore, overexpression of PANDER from the pancreatic β-cell decreases hepatic p-AMPK signaling and to a limited extent provides a potential mechanism for the observed increased lipogenesis and gluconeogenesis within this model.

http://joe.endocrinology-journals.org
DOI: 10.1530/JOE-13-0338

Published by Bioscientifica Ltd.

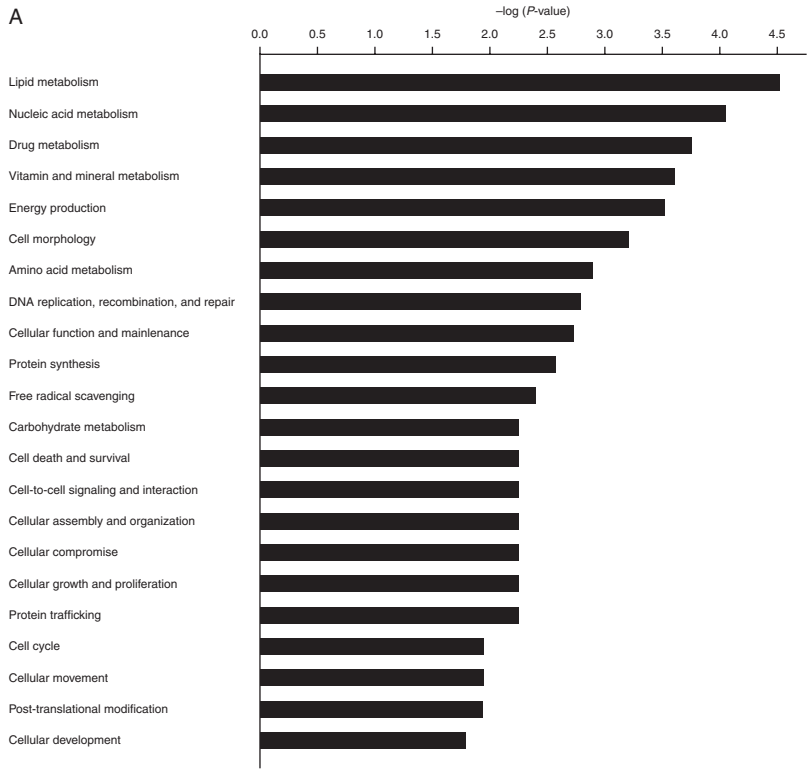

B

Increased PANTG hepatic proteins	Fold change above WT
FABP1	2.8
PKA	2.8
PEPCK	3.5
SCP2	3.5
ACSL1	4.6
ENTPD5	8.3

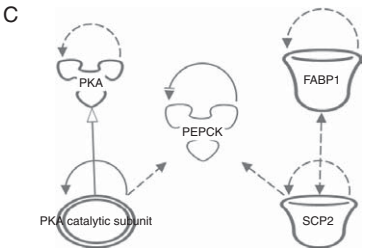

Figure 5
Stable isotope labeling of amino acids in cell culture (SILAC) analysis of PANTG. Total protein isolate was prepared from isolated livers from PANTG and WT mice ($n=6$ per group) obtained during fed conditions. Following processing and SILAC analysis, 1640 proteins were identified and quantitated. Data were normalized and analyzed using the Ingenuity Pathway Analysis (IPA) program. Relative changes in the levels of identified proteins were determined by the ratio of PANTG to that of WT and normalized to Tubulin B5. (A) IPA analysis of predicted impacted metabolic functions indicates lipid metabolism is altered in PANTG liver. (B) Differentially expressed hepatic proteins identified in PANTG and predicted to increase triglyceride production. (C) Network analysis of differentially expressed proteins involved in triglyceride production demonstrated to functionally interact as indicated by lines.

Discussion

The hallmark characteristics of our PANTG model in younger male mice demonstrated the following: 1) increased fasting hyperglycemia and insulinemia, 2) impaired glucose tolerance, 3) increased hepatic insulin resistance, 4) increased proteomic profile of lipogenesis and gluconeogenesis, 5) increased hepatic triglyceride content, 6) decreased hepatic glycogen, and 7) decreased p-AMPK signaling. These findings strongly suggest that pancreas-specific PANDER can alter glycemic levels through what appears to be a specific interaction with the liver and impact phosphorylation of critical downstream hepatic signaling molecules such as AMPK. The generation and evaluation of the pancreas-specific PANDER overexpressing transgenic mouse allowed us to evaluate the physiologic effects of secreted PANDER and the impact on glycemic and lipid modulation.

To put our data in the context of other published *in-vivo* studies, we compared our results to the overall findings of others, albeit this comparison was made to acute models (Table 1). The two other published studies utilized tail vein-injected adenoviral-delivered PANDER to induce a hepatic overexpression of PANDER (Wilson *et al.* 2010, Li *et al.* 2011). Some of the earliest reports detailing the localization of PANDER did not find any expression in the liver (Zhu *et al.* 2002), but recently others have surfaced to demonstrate that PANDER is expressed within this organ as well and is consistent with our findings (Li *et al.* 2011, 2013, Mou *et al.* 2013). Therefore, there is definitive physiological relevance to this approach but does not take into account the biological influence of pancreas-specific PANDER. Both prior studies evaluated the impact of Ad-PANDER following either 3 (Li *et al.* 2011) or 7 days (Wilson *et al.* 2010) post viral

http://joe.endocrinology-journals.org
DOI: 10.1530/JOE-13-0338

Published by Bioscientifica Ltd.

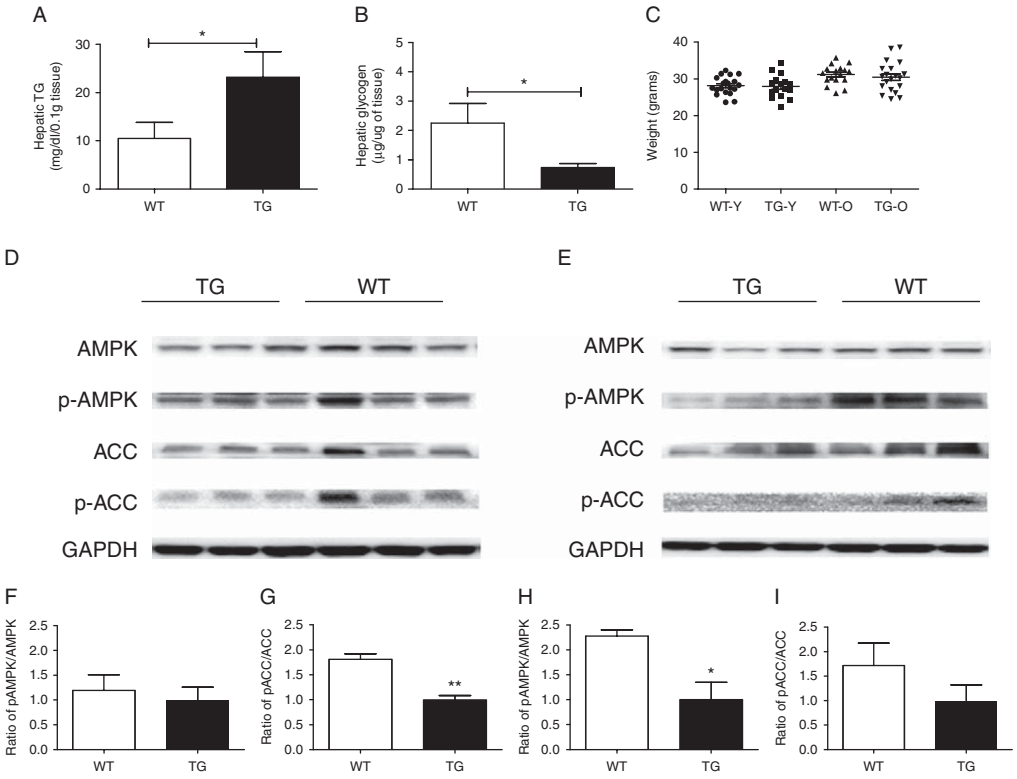

Figure 6
Characterization of PANTG liver. (A) Hepatic triglyceride (TG) content measured from male PANTG livers during fasting conditions ($n=4$). (B) Hepatic glycogen content of male PANTG livers during fasting conditions ($n=6$–8). (C) Body weight (g) measured from young and old PANTG and WT mice ($n=18$–20). Values are expressed as means±S.E.M. *$P<0.05$ by Student's *t*-test. (D) Western analysis of total AMPK, phosphorylated AMPK, ACC, and phosphorylated AMPK from liver lysates of fasting male PANTG and WT mice. Lanes 1–3 and 4–6 are from PANTG and WT mice, respectively ($n=3$). (E) Western analysis from liver lysates from insulin-stimulated (2 U/kg) PANTG and WT mice as described in D. (F, G, H, and I) Densitometric analysis by ImageJ of western blots evaluating ratio of phosphorylated AMPK and ACC normalized to total levels and GAPDH expressed as relative to PANTG. (F) AMPK fasting conditions, (G) ACC fasting conditions, (H) AMPK insulin stimulated conditions, and (I) ACC insulin stimulated conditions. *$P<0.05$ and *$P<0.01$ by Student's *t*-test.

administration. There were numerous differences in phenotypic observations between these prior studies that included fasting glycemia, corticosterone levels, glucose tolerance, hepatic triglycerides, and intracellular hepatic signaling such as with AMPK. Our findings appeared to strongly complement the overall but sometimes contrasting data presented from both studies in that observations that were identified in a single acute study were also identified with the PANTG (Table 1). Taken together, this may indicate overlapping roles between hepatic and pancreatic-specific PANDER that may complement each other and provide a synergistic effect on glycemic levels and hepatic insulin sensitivity. In combination with the findings from the *Pander* knockout mouse, PANDER may serve distinct biological roles in the regulation of glycemic levels. The previously reported PANKO mouse displayed impaired insulin secretion and glucose tolerance due to abnormal calcium signaling within the pancreatic islets. However, this model also demonstrated enhanced hepatic insulin signaling along with decreased HGP during HEC studies. The previous knockout results in addition to our currently presented transgenic study allude to the pleiotropic nature of this novel class of hormones with regard to biological action within pancreatic β-cell and hepatic metabolic pathways. Furthermore, PANDER may even serve a function in cell survival as there is extensive literature supporting that PANDER has a pro-apoptotic effect on pancreatic islets *in vitro* (Cao *et al.* 2003, 2005, Yang *et al.* 2005). However, this study did not reveal any increased pancreatic islet apoptosis by 5-bromo-2-deoxyuridine staining (data not shown). This discrepancy between experimental observations may be attributed to compensatory mechanisms present *in vivo* that may promote cell survival or the levels of PANDER overexpression within this model are not sufficiently high enough to induce apoptosis.

http://joe.endocrinology-journals.org
DOI: 10.1530/JOE-13-0338

Published by Bioscientifica Ltd.

Table 1 Summary of phenotypic observations from PANDER acute and transgenic models. Acute model 1 and 2 results are derived from Wilson *et al.* (2010) and Li *et al.* (2011), respectively. PANTG describes summary of results from currently described study

Phenotype	Acute model 1	Acute model 2	PANTG
↑ Fasting glycemia	X	No	X
↑ Fasting insulinemia	X	X	X
↑ Corticosterone	X	No	No
↑ Glucagon	No	No	No
Glucose intolerance	X	No	X
Insulin intolerance	No	No	No
↑ HGP	NE	NE	X
↑ Hepatic triglycerides	No	X	X
↓ Hepatic glycogen	No	No	X
↓ p-AMPK	No	X	X

X, presence; No, absence; NE, not evaluated.

A distinguishing trait among all PANDER models is the increase in fasting hyperinsulinemia as compared with WT controls (Table 1). This observation may be the result of either increased pancreatic β-cell secretion, impaired insulin sensitivity, or compensatory consequence of increased fasting glycemia. Data from others and investigations from our laboratory (data not shown) certainly indicate impaired hepatic insulin sensitivity with mild to no impact of PANDER overexpression on pancreatic β-cell secretion insulin secretion. In contrast, the *Pander* knockout on mixed genetic background has demonstrated impaired insulin secretion with decreased glucose-stimulated intracellular calcium signaling, providing evidence of a pleiotropic role of PANDER in islets as well as liver (Robert-Cooperman *et al.* 2010). However, in the context of our transgenic and the acute models, the increased fasting hyperinsulinemia appears to be attributed to decreased hepatic but not peripheral insulin sensitivity. Our HEC studies have provided some of the strongest data supporting this conclusion and exhibited no significant differences in GIR and rate of disappearance but increased HGP (Fig. 4C). This elevated HGP can also be the result of increased circulating hormones such as glucagon or corticosterones that can enhance cAMP and CREB signaling (Dirlewanger *et al.* 2000, Jiang & Zhang 2003). However, our study did not demonstrate any altered levels in corticosteroids or glucagon and indicate that the elevated HGP is attributed to hepatic insulin resistance along with the selective PANDER-induced effects.

Type 2 diabetes (T2D) is characterized by insulin resistance in a multitude of tissues, resulting in a compensatory or consequential physiological condition of the typical T2D metabolic triad of hyperinsulinemia, hyperglycemia, and hypertriglyceridemia (Muoio & Newgard 2008). Hepatic insulin resistance is a major component of T2D, resulting in decreased suppression of HGP due to blunted insulin signaling (Saad *et al.* 1992, Kerouz *et al.* 1997). However, there is a major uncharacterized detrimental paradox with hepatic insulin resistance in T2D that has yet to be elucidated in that it is selective rather than total (Brown & Goldstein 2008). Despite impaired insulin signaling, hepatic lipogenesis is increased resulting in excessive production of fatty acid synthesis and triglyceride accumulation, resulting in a highly detrimental condition and promotion of metabolic syndrome and further insulin resistance. Total insulin resistance in the liver-specific insulin receptor knockout (LIRKO) mouse demonstrated that insulin fails to decrease gluconeogenesis and synthesis of fatty acids, indicating that this is a less severe metabolic defect than selective hepatic insulin resistance (SHIR; Biddinger *et al.* 2008). The precise mechanism and cofactors responsible for the onset and progression of SHIR are unknown. Taken together, the PANTG demonstrates a SHIR-like phenotype due to simultaneous presence of hepatic insulin resistance with increased HGP and lipogenesis. HEC and SILAC results together provide the evidence of increased HGP and PEPCK expression with a stimulation of triglyceride production and provide potentially novel pathways for the onset of SHIR. One potential conclusion is that PANDER may serve as a cofactor in the onset of SHIR in T2D. Experiments evaluating the secretagogues of PANDER strongly implicate that hallmark T2D conditions of hyper-glycemia, insulinemia, and lipidemia would promote PANDER expression (Burkhardt *et al.* 2005, Yang *et al.* 2005, Wang *et al.* 2008, Li *et al.* 2011). Three recent reviews have arrived at similar conclusions implicating PANDER in the onset and progression of hepatic insulin resistance in T2D and potentially nonalcoholic fatty liver disease (Wilson *et al.* 2011, Wang *et al.* 2012, Yang & Guan 2013). Further extensive studies evaluating subjects with and without T2D in context of PANDER levels are needed to fully warrant this conclusion.

Proteomics by SILAC analysis revealed upregulation of a network of key genes related to gluconeogenesis and lipogenesis, specifically *PEPCK*, *FABP1*, *PRKAR2B*, *SCP2*, *ACSL1*, and *ENTPD5*. *PEPCK* controls the rate limiting step in gluconeogenesis and suppression is expected under conditions of hyperglycemia and insulin secretion (Hanson & Reshef 1997). *ACSL1* is an isozyme of the long-chain fatty-acid-coenzyme A ligase family that convert

http://joe.endocrinology-journals.org
DOI: 10.1530/JOE-13-0338

Published by Bioscientifica Ltd.

free long-chain fatty acids into fatty acyl-CoA esters, and serve a central role in lipid biosynthesis (Ning *et al.* 2011). Proteins of FABP1 and SCP2 serve as binding and carrier proteins involved in lipid homeostasis (Amigo *et al.* 2003, Newberry *et al.* 2003), PRKAR2B and ENTPD5 are involved in the substrate production necessary for lipogenesis (Schreyer *et al.* 2001, Read *et al.* 2009). In addition, AMPK is known to have numerous effects upon hepatic metabolism, including inhibition of gluconeogenesis, lipogenesis, and glycogen production (Canto & Auwerx 2010). In particular, activation of AMPK decreases hepatic triglyceride production by increasing β oxidation in the cell (Winder & Hardie 1999). Concordantly, we observed decreased p-AMPK upon insulin stimulation with an observed increase in glycogen production and hepatic triglycerides. During pathological conditions, PANDER may promote SHIR by disrupting activation and phosphorylation of p-AMPK. AMPK inhibits ACC, an enzyme responsible for the synthesis of malonyl-CoA that results in increased triglyceride synthesis. Our results in the PANTG are consistent with decreased p-AMPK and p-ACC resulting in increased hepatic triglyceride production. Further studies are needed and ongoing to elucidate the PANDER receptor and additional signaling molecules impacted by PANDER-induced inhibition of p-AMPK.

In summary, the generation and characterization of the PANTG reveals that pancreas-secreted PANDER serves a selective role in the counter-regulation of hepatic insulin action by impairing insulin-induced suppression of gluconeogenesis but by promoting hepatic triglyceride production under typical physiological conditions. However, under pathological conditions such as in T2D, PANDER may impart SHIR and serve as a co-factor driving a detrimental cycle of hepatic insulin resistance.

Declaration of interest

The authors declare that there is no conflict of interest that could be perceived as prejudicing the impartiality of the review.

Funding

This work was partially supported by the USF New Investigator Award to B R B.

Acknowledgements

The authors thank Moffitt Stabile vivarium for assistance with animal care and director Dr Rex Ahima of the University of Pennsylvania Mouse Phenotyping, Physiology, and Metabolism Core.

References

Amigo L, Zanlungo S, Miquel JF, Glick JM, Hyogo H, Cohen DE, Rigotti A & Nervi F 2003 Hepatic overexpression of sterol carrier protein-2 inhibits VLDL production and reciprocally enhances biliary lipid secretion. *Journal of Lipid Research* **44** 399–407. (doi:10.1194/jlr.M200306-JLR200)

Aurora R & Rose GD 1998 Seeking an ancient enzyme in *Methanococcus jannaschii* using ORF, a program based on predicted secondary structure comparisons. *PNAS* **95** 2818–2823. (doi:10.1073/pnas.95.6.2818)

Biddinger SB, Hernandez-Ono A, Rask-Madsen C, Haas JT, Aleman JO, Suzuki R, Scapa EF, Agarwal C, Carey MC, Stephanopoulos G *et al.* 2008 Hepatic insulin resistance is sufficient to produce dyslipidemia and susceptibility to atherosclerosis. *Cell Metabolism* **7** 125–134. (doi:10.1016/j.cmet.2007.11.013)

Brown MS & Goldstein JL 2008 Selective versus total insulin resistance: a pathogenic paradox. *Cell Metabolism* **7** 95–96. (doi:10.1016/j.cmet.2007.12.009)

Burkhardt BR, Yang MC, Robert CE, Greene SR, McFadden KK, Yang J, Wu J, Gao Z & Wolf BA 2005 Tissue-specific and glucose-responsive expression of the pancreatic derived factor (PANDER) promoter. *Biochimica et Biophysica Acta* **1730** 215–225. (doi:10.1016/j.bbaexp.2005.07.003)

Burkhardt BR, Cook JR, Young RA & Wolf BA 2008 PDX-1 interaction and regulation of the Pancreatic Derived Factor (PANDER, FAM3B) promoter. *Biochimica et Biophysica Acta* **1779** 645–651. (doi:10.1016/j.bbagrm.2008.07.007)

Canto C & Auwerx J 2010 AMP-activated protein kinase and its downstream transcriptional pathways. *Cellular and Molecular Life Sciences* **67** 3407–3423. (doi:10.1007/s00018-010-0454-z)

Cao X, Gao Z, Robert CE, Greene S, Xu G, Xu W, Bell E, Campbell D, Zhu Y, Young R *et al.* 2003 Pancreatic-derived factor (FAM3B), a novel islet cytokine, induces apoptosis of insulin-secreting β-cells. *Diabetes* **52** 2296–2303. (doi:10.2337/diabetes.52.9.2296)

Cao X, Yang J, Burkhardt BR, Gao Z, Wong RK, Greene SR, Wu J & Wolf BA 2005 Effects of overexpression of pancreatic derived factor (FAM3B) in isolated mouse islets and insulin-secreting βTC3 cells. *American Journal of Physiology. Endocrinology and Metabolism* **289** E543–E550. (doi:10.1152/ajpendo.00113.2005)

Carnegie JR, Robert-Cooperman CE, Wu J, Young RA, Wolf BA & Burkhardt BR 2010 Characterization of the expression, localization, and secretion of PANDER in α-cells. *Molecular and Cellular Endocrinology* **325** 36–45. (doi:10.1016/j.mce.2010.05.008)

Chen S, Cao XP, Xiao HP & Li YB 2011 Effects of glucagon-like peptide-1 on the free fatty acid-induced expression of pancreatic derived factor in cultured beta-TC3 cell line. *Zhonghua Yi Xue Za Zhi* **91** 1413–1416.

Dirlewanger M, Schneiter PH, Paquot N, Jequier E, Rey V & Tappy L 2000 Effects of glucocorticoids on hepatic sensitivity to insulin and glucagon in man. *Clinical Nutrition* **19** 29–34. (doi:10.1054/clnu.1999.0064)

Hanson RW & Reshef L 1997 Regulation of phosphoenolpyruvate carboxykinase (GTP) gene expression. *Annual Review of Biochemistry* **66** 581–611. (doi:10.1146/annurev.biochem.66.1.581)

Jiang G & Zhang BB 2003 Glucagon and regulation of glucose metabolism. *American Journal of Physiology. Endocrinology and Metabolism* **284** E671–E678. (doi:10.1152/ajpendo.00492.2002)

Johansson P, Bernstrom J, Gorman T, Oster L, Backstrom S, Schweikart F, Xu B, Xue Y & Schiavone LH 2013 FAM3B PANDER and FAM3C ILEI represent a distinct class of signaling molecules with a non-cytokine-like fold. *Structure* **21** 306–313. (doi:10.1016/j.str.2012.12.009)

Kerouz NJ, Horsch D, Pons S & Kahn CR 1997 Differential regulation of insulin receptor substrates-1 and -2 (IRS-1 and IRS-2) and phosphatidylinositol 3-kinase isoforms in liver and muscle of the obese diabetic (ob/ob) mouse. *Journal of Clinical Investigation* **100** 3164–3172. (doi:10.1172/JCI119872)

Kruger M, Kratchmarova I, Blagoev B, Tseng YH, Kahn CR & Mann M 2008 Dissection of the insulin signaling pathway via quantitative

http://joe.endocrinology-journals.org
DOI: 10.1530/JOE-13-0338

Published by Bioscientifica Ltd.

phosphoproteomics. *PNAS* **105** 2451–2456. (doi:10.1073/pnas.0711713105)

Li J, Chi Y, Wang C, Wu J, Yang H, Zhang D, Zhu Y, Wang N, Yang J & Guan Y 2011 Pancreatic-derived factor promotes lipogenesis in the mouse liver: role of the forkhead box 1 signaling pathway. *Hepatology* **53** 1906–1916. (doi:10.1002/hep.24295)

Li Z, Mou H, Wang T, Xue J, Deng B, Qian L, Zhou Y, Gong W, Wang JM, Wu G *et al.* 2013 A non-secretory form of FAM3B promotes invasion and metastasis of human colon cancer cells by upregulating Slug expression. *Cancer Letters* **328** 278–284. (doi:10.1016/j.canlet.2012.09.026)

Melloul D, Marshak S & Cerasi E 2002 Regulation of pdx-1 gene expression. *Diabetes* **51**(Suppl 3) S320–S325. (doi:10.2337/diabetes.51.2007.S320)

Monetti M, Nagaraj N, Sharma K & Mann M 2011 Large-scale phosphosite quantification in tissues by a spike-in SILAC method. *Nature Methods* **8** 655–658. (doi:10.1038/nmeth.1647)

Mou H, Li Z, Yao P, Zhuo S, Luan W, Deng B, Qian L, Yang M, Mei H & Le Y 2013 Knockdown of FAM3B triggers cell apoptosis through p53-dependent pathway. *International Journal of Biochemistry & Cell Biology* **45** 684–691. (doi:10.1016/j.biocel.2012.12.003)

Muoio DM & Newgard CB 2008 Mechanisms of disease: molecular and metabolic mechanisms of insulin resistance and β-cell failure in type 2 diabetes. *Nature Reviews. Molecular Cell Biology* **9** 193–205. (doi:10.1038/nrm2327)

Newberry EP, Xie Y, Kennedy S, Han X, Buhman KK, Luo J, Gross RW & Davidson NO 2003 Decreased hepatic triglyceride accumulation and altered fatty acid uptake in mice with deletion of the liver fatty acid-binding protein gene. *Journal of Biological Chemistry* **278** 51664–51672. (doi:10.1074/jbc.M309377200)

Ning J, Hong T, Yang X, Mei S, Liu Z, Liu HY & Cao W 2011 Insulin and insulin signaling play a critical role in fat induction of insulin resistance in mouse. *American Journal of Physiology. Endocrinology and Metabolism* **301** E391–E401. (doi:10.1152/ajpendo.00164.2011)

Read R, Hansen G, Kramer J, Finch R, Li L & Vogel P 2009 Ectonucleoside triphosphate diphosphohydrolase type 5 (Entpd5)-deficient mice develop progressive hepatopathy, hepatocellular tumors, and spermatogenic arrest. *Veterinary Pathology* **46** 491–504. (doi:10.1354/vp.08-VP-0201-R-AM)

Robert-Cooperman CE, Carnegie JR, Wilson CG, Yang J, Cook JR, Wu J, Young RA, Wolf BA & Burkhardt BR 2010 Targeted disruption of pancreatic-derived factor (PANDER, FAM3B) impairs pancreatic β-cell function. *Diabetes* **59** 2209–2218. (doi:10.2337/db09-1552)

Saad MJ, Araki E, Miralpeix M, Rothenberg PL, White MF & Kahn CR 1992 Regulation of insulin receptor substrate-1 in liver and muscle of animal models of insulin resistance. *Journal of Clinical Investigation* **90** 1839–1849. (doi:10.1172/JCI116060)

Samaras SE, Cissell MA, Gerrish K, Wright CV, Gannon M & Stein R 2002 Conserved sequences in a tissue-specific regulatory region of the pdx-1 gene mediate transcription in pancreatic β cells: role for hepatocyte nuclear factor 3 β and Pax6. *Molecular and Cellular Biology* **22** 4702–4713. (doi:10.1128/MCB.22.13.4702-4713.2002)

Schreyer SA, Cummings DE, McKnight GS & LeBoeuf RC 2001 Mutation of the RIIβ subunit of protein kinase A prevents diet-induced insulin resistance and dyslipidemia in mice. *Diabetes* **50** 2555–2562. (doi:10.2337/diabetes.50.11.2555)

Wang O, Cai K, Pang S, Wang T, Qi D, Zhu Q, Ni Z & Le Y 2008 Mechanisms of glucose-induced expression of pancreatic-derived factor in pancreatic β-cells. *Endocrinology* **149** 672–680. (doi:10.1210/en.2007-0106)

Wang C, Burkhardt BR, Guan Y & Yang J 2012 Role of pancreatic-derived factor in type 2 diabetes: evidence from pancreatic β cells and liver. *Nutrition Reviews* **70** 100–106. (doi:10.1111/j.1753-4887.2011.00457.x)

Wilson CG, Schupp M, Burkhardt BR, Wu J, Young RA & Wolf BA 2010 Liver-specific overexpression of pancreatic-derived factor (PANDER) induces fasting hyperglycemia in mice. *Endocrinology* **151** 5174–5184. (doi:10.1210/en.2010-0379)

Wilson CG, Robert-Cooperman CE & Burkhardt BR 2011 PANcreatic-DERived factor: novel hormone PANDERing to glucose regulation. *FEBS Letters* **585** 2137–2143. (doi:10.1016/j.febslet.2011.05.059)

Winder WW & Hardie DG 1999 AMP-activated protein kinase, a metabolic master switch: possible roles in type 2 diabetes. *American Journal of Physiology* **277** E1–E10.

Xiang JN, Chen DL & Yang LY 2012 Effect of PANDER in betaTC6-cell lipoapoptosis and the protective role of exendin-4. *Biochemical and Biophysical Research Communications* **421** 701–706. (doi:10.1016/j.bbrc.2012.04.065)

Yang J & Guan Y 2013 Family with sequence similarity 3 gene family and nonalcoholic fatty liver disease. *Journal of Gastroenterology and Hepatology* **28**(Suppl 1) 105–111. (doi:10.1111/jgh.12033)

Yang J, Robert CE, Burkhardt BR, Young RA, Wu J, Gao Z & Wolf BA 2005 Mechanisms of glucose-induced secretion of pancreatic-derived factor (PANDER or FAM3B) in pancreatic β-cells. *Diabetes* **54** 3217–3228. (doi:10.2337/diabetes.54.11.3217)

Zhu Y, Xu G, Patel A, McLaughlin MM, Silverman C, Knecht K, Sweitzer S, Li X, McDonnell P, Mirabile R *et al.* 2002 Cloning, expression, and initial characterization of a novel cytokine-like gene family. *Genomics* **80** 144–150. (doi:10.1006/geno.2002.6816)

Received in final form 3 December 2013
Accepted 12 December 2013

http://joe.endocrinology-journals.org
DOI: 10.1530/JOE-13-0338

Published by Bioscientifica Ltd.